*Chem Biol Drug Des 2008;* **71:** 197–204

Research Article



doi: 10.1111/j.1747-0285.2008.00630.x

# Conformational Movement of F251 Contributes to the Molecular Mechanism of Constitutive Activation in the C5a Receptor

**Saurabh Sen[1,‡], Thomas J. Baranski[1] and Gregory V. Nikiforovich[2,*]**

*[1]Division of Endocrinology, Metabolism and Lipid Research, Department of Internal Medicine, Washington University School of Medicine, Box 8127, St Louis, MO 63110, USA*
*[2]Department of Biochemistry and Molecular Biophysics, Washington University School of Medicine, Box 8036, St Louis, MO 63110, USA*
*[‡]Present address: Center for Neurodegeneration and Experimental Therapeutics, Department of Neurology, University of Alabama at Birmingham, 1719 6th Ave. S, Birmingham, AL 35294, USA*
**Corresponding author: Gregory V. Nikiforovich, gregory@ccb.wustl.edu*

**The activation mechanism of G-protein-coupled receptors triggered upon binding of a ligand represents a very important 'conformational switch' in the biological array of signal transduction. However, the molecular and functional details for this activation switch remain unknown. Random saturation mutagenesis data on the complement factor 5a receptor has provided a large data set of mutants including several constitutively active mutants. In the present study, we employed computational modeling to rationalize the constitutive activity for two constitutively active mutants, NQ (I124N/L127Q) and F251A, and we then made predictions for a series of mutants that either promote or constrain constitutive activity. Biological testing of the site-directed mutants confirmed most of the predictions of the computational modeling. These results support a molecular mechanism of constitutive activity in complement factor 5a receptor mutants that is associated with conformational changes in a network of residues neighboring F251 as the focal point of origin.**

**Key words:** complement factor 5a receptor, constitutive activity, G-protein-coupled receptors, molecular modeling, mutant receptors

**Abbreviations:** GPCR, G-protein-coupled receptor; TM, transmembrane helix; CAM, constitutively active mutant; RSM, random saturation mutagenesis; PDB, protein data bank; W5Cha, Me-Phe-Lys-Pro-D-Cha-Cha-D-Arg; D-Cha, D-cyclohexylalanine; C5a, complement factor 5a

Received 14 December 2007, revised and accepted for publication 2 January 2008

G-protein-coupled receptors (GPCRs) are membrane-bound cell surface receptors involved in communication between the external environment and biological information machinery housed within the cell. They comprise a superfamily with more than 800 members (1,2) and constitute one of the largest subclasses of the human genome. It is estimated that *ca.* 40% of all present day drugs act through these receptors (3), thus illustrating their promise as targets for the pharmaceutical industry. G-protein-coupled receptors are integral membrane proteins, and include seven helical transmembrane (TM) stretches as well as non-TM parts, namely the N- and C-terminal fragments and the extracellular and intracellular loops connecting the TM helices.

Upon ligand stimulation, GPCRs undergo a conformational change from their resting states (the R states) to the activated states (the R* states) to attain the active state conformation. It is in this active conformation that the signaling machinery is turned on resulting in intracellular protein activation. How a small molecule ligand can lead to such a conformational change remains to be the unanswered question in this activation machinery. One way of addressing this problem is to identify and generate constitutively active mutants (CAMs), which are believed to exist in an active conformation resulting in production of second messenger, even in the absence of an agonist. The 'constitutive activity' is a gain-of-function phenotype and is defined as the number of receptors spontaneously adopting an active conformation, which cannot be measured directly (4). Therefore, CAMs may be convenient models for studying the activated states of GPCRs (5) given that CAMs mimic the active conformations of GPCRs. This assumption was the main rationale for the present study. Another assumption was that the R and R* states likely do not differ significantly in their relative energies, as binding of a ligand, which is normally of much smaller size than a GPCR, cannot force the GPCR to adopt a conformation of significantly higher overall energy. This should be especially true for CAMs; indeed, energy calculations performed for rhodopsin and its CAMs confirmed this suggestion (6).

The CAM receptors have become useful experimental tools in studying the activation process in the absence of agonists, while their increased affinity and efficacy for agonists is an advantage for ligand screening (7). There has been much work and discussion on the constitutive activity of GPCRs including the conceptual framework of the constitutive activity in GPCRs (8,9), insights into structural basis for constitutive activation (10,11), theoretical basis of activation (2,12–14), and the disease states related to constitutively active receptors (15). Deciphering the molecular mechanism for con-

stitutive activation would shed light on the receptor activation mechanism as well as have a great impact on drug discovery.

In this study, we have applied previously developed procedures of molecular modeling (6,16,17) for rational design of CAMs of the complement factor 5a receptor (C5aR), a rhodopsin-like GPCR expressed primarily on the surface of neutrophils and other myeloid cells. This receptor has been fully investigated by random saturation mutagenesis (RSM) in the yeast system (18–20). The RSM analyses focused on the TM regions of C5aR elucidated several CAMs in the yeast system, mostly due to mutations in TM helices 3 and 6 (TM3 and TM6; 18,19). Two of the CAMs, namely NQ (I124N/L127Q) and F251A, showed high basal activity also in the mammalian cells (21). In addition, a complementing mutation (N296A) restored ligand-dependent signaling in the NQ-mutated C5aR expressed in mammalian cells (21). Thus, NQ and F251A are the only two known CAMs of C5aR in the mammalian system obtained by point mutations in the TM region of C5aR.

In the present study, we asked: (i) which conformational changes of side chains (if any) are most characteristic for CAMs and (ii) which novel mutations will stimulate conformational changes associated with constitutive activity? We have used molecular modeling to reveal conformational changes occurring in the TM region of the C5aR as a result of NQ and F251A mutations to probe for the possible molecular mechanism of constitutive activity, and to design mutations presumably enhancing/impairing the corresponding conformational changes. The designed mutants were then tested in the mammalian system to validate predictions from molecular modeling.

## Methods

### *Molecular modeling*

The 3D structure of the TM regions of C5aR was modeled by the same energy calculation procedure described elsewhere (20,22). Briefly, the procedure of packing the TM helical bundle minimized the sum of all intrahelical and interhelical interatomic energies in the multidimensional space of parameters that included 'global' parameters (those related to movements of individual helices as rigid bodies) and 'local' parameters (the dihedral angles of the side chains for all helices). The extracellular and intracellular loops as well as the N-terminal and C-terminal non-TM fragments of C5aR were not modeled. The dihedral angles of the side chains for all helices were optimized (repacked) prior to energy minimization according to the algorithm developed earlier (23). The 'global' starting point for the TM bundle corresponding to the resting R state of C5aR was selected by spatial alignment of TM helices onto the X-ray structure of rhodopsin (the PDB entry 1F88, chain A). Energy minimization that started from these global parameters yielded a 3D structure of the TM bundle differing from that of 1F88 by the rms value of 2.40 Å (Cα-atoms only). Energy calculations for the C5aR mutant receptors were performed exactly as for C5aR itself. For each receptor, including the wild type, two runs of energy minimization were performed. They differed by the starting dihedral angle $\chi_1$ for F251, which value was selected as either *ca.* 180/ (*trans*-rotamer, *t*) or *ca.* –60/ (gauche-minus rotamer, *g*–). This particular dihedral angle was excluded from procedure of repacking side chains according to Ref. (23) prior to energy minimization, but it was involved in the subsequent process of energy minimization.

### *Biological studies*

#### Generation of mutants

The mutants used in this study were generated from wild-type eGFP-tagged C5aR by site-directed mutagenesis (Pfu turbo mutagenesis; Strategene, La Jolla, CA, USA) using homologous recombination in yeast BY1142. Mutants were first screened using fluorescence and further confirmed with sequencing at the Washington University Protein and Nucleic Acid Chemistry Laboratory. Cloning in the mammalian vector was carried out by a simple step of restriction endonuclease digestion and ligation after introducing the restriction sites through a PCR. The clones in the mammalian vector were confirmed with restriction mapping with an internal restriction site.

#### Inositol phosphate accumulation measurement

Activation of PLC$\beta$ by C5aR requires the presence of human G$\alpha_{16}$. For all the inositol phosphate (IP) measurements in the current study the G$\alpha_{16}$ [in pcDNA3.1(+)] was co-transfected along with the DNA constructs into COS-7 cells with Lipofectamine 2000 (Invitrogen Inc., Carlsbad, CA, USA), according to the manufacturer's instructions. Cells were treated with 1 $\mu$M W5Cha (GenScript, Piscataway, NJ, USA) or no ligand, and $IP_3$ levels were measured as previously described (24). Radioactive counts were determined in Scintiverse scintillation fluid (Fisher, Fair Lawn, NJ, USA) and the counts were recorded until 5% significance. The data are represented as the ratio of $IP_3$ to total inositol (fraction 3/fraction 1 + fraction 3) × 100. Curve fitting was performed with PRISM v 4.0 (GraphPad Software, San Diego, CA, USA). Statistical significance was determined using a one-way analysis of variance test with Dunnett's post-test and a 95% confidence level.

#### Electrophoresis and Western blotting

COS-7 cells transfected with the various constructs (under same conditions as in case of IP assay) were used for the expression studies. The cells were lysed with 1X SDS sample buffer (50 mM Tris, pH 6.8, 2% SDS and 10% glycerol) supplemented with 2% $\beta$-mercaptoethanol, 1 $\mu$g/mL leupeptin, 1 $\mu$g/mL aprotinin, and 500 $\mu$M phenylmethysulfonyl fluoride by aspirating through a 27-gauge needle 10 times. The samples were analyzed on a 12% SDS-PAGE and electro-transferred onto nitrocellulose membranes for Western blotting. For immunostaining, polyclonal C5aR primary antibody (raised against a peptide corresponding to the N-terminus) was used and the signal was detected using horseradish peroxidase-conjugated anti-rabbit antibody (1:10 000) for $IgG_1$ (Santa Cruz Biotechnology, Santa Cruz, CA, USA) followed by chemiluminescence (Roche, Palo Alto, CA, USA).

#### Binding assay

Binding assays on isolated membranes were performed using [$^{125}$I]-C5a (40 $\mu$Ci/mL; Perkin-Elmer, Waltham, MA, USA) as a radioligand. Using the membranes prepared, the binding assays included

5 $\mu$g of total protein for each data point. After the membranes were thawed on ice, the protein concentration was determined using BSA as standard. The binding reaction was set up using the Binding Buffer (Hanks buffer, 25 mM HEPES, pH 7.5, BSA 0.1%) containing the membrane fraction and cold C5a (concentration varying between $10^{-11}$ and $10^{-5}$). The reaction was initiated upon addition of 100 pM of [$^{125}$I]-C5a. After incubation for 45 min, the reaction was terminated through filtration with a Millipore (Temecula, CA, USA) harvester using GF/C filter presoaked in Binding Buffer containing 0.1% poly(ethylenimine) (Sigma, St. Louis, MO, USA). Upon three rounds of washing, the filters were dried, folded into quarters and added to scintillation tubes with 3 mL of the scintillation liquid.

## Results

### *Molecular modeling*

We have modeled the 3D structure of the TM region of C5aR in the resting R state by homology to the X-ray structure of rhodopsin (the PDB entry 1F88), as described in Methods. The same 3D model was employed by us earlier, where we have revealed the unique structural role of the side chain of the conserved F251 residue in maintaining the network of interactions between the functionally essential (preserved) residues in C5aR determined by the RSM (22). Specifically, the residues that are both preserved in C5aR and conserved in the rhodopsin-like family of GPCRs form two clusters of residues in close contact (defined as a distance of <5 Å between at least one pair of atoms belonging to the side chains of contacting residues). The two clusters are connected through interactions between residues F251 in TM6 with S123 and L126 in TM3 as well as with N296 in TM7 (22). The side chain of F251 is in close contact not only with the preserved residues S123, L126, and N296, but, depending on the particular rotamer of the side chain, also with the side chains of residues I124, L127 (TM3), V247, F254, W255 (TM6), and N292 (TM7). In this model, F251 contacts residues that when mutated (I124N/L127Q in the NQ mutant) evoke constitutive activity; in addition, an alanine substitution at F251 results in a pronounced CAM. Combined, these findings suggest that residues in the vicinity of F251 may form a hot spot for designing new CAMs of C5aR.

Figure 1A displays the lowest energy conformation of the wild-type C5aR found by our energy calculations. In this conformation, the side chain of F251 was placed on the interface between TM3, TM6, and TM7 (shown as white shadowed ribbons), which corresponded to the *g*– rotamer of F251. In the F251A mutant, which is a pronounced CAM, the bulky side chain of F251 was replaced with a much smaller alanine and, therefore, was effectively eliminated from the TM6/TM7 interface. Significant constitutive activity was also observed in the NQ mutant, where the bulky aliphatic residues I124 and L127 that are close to F251 were replaced by the less voluminous and more flexible N124 and Q127, respectively. The net effect of these substitutions may result in movement of the F251 side chain from rotamer *g*– to rotamer *t* upon which F251 enters the pocket formed by residues Q127 and N124 in TM3 and F254 and W255 in TM6 (Figure 1B). This 'conformational switch' would allow the side chain of F251 to clear the TM6/TM7 interface thus allowing possible rotations of both helices, which may accompany conformational transitions from R to R*. These observations imply that the 'activation switch mechanism' involves the conformational transition of the F251 side chain from one rotamer (Figure 1A) to another (Figure 1B), and suggests that mutations that facilitate this rotations would trigger constitutive activity in the C5aR mutants.

To achieve this transition to the active state, the side chain of F251 should enter the pocket formed by residues L127 and I124 in TM3 and F254 and W255 in TM6. The residues L127 and F254 gate the pocket preventing the side chain of F251 from entering. Therefore, elimination of the side chains of L127 and/or F254 could facilitate possible entering of the F251 side chain in the pocket. Also, elimination of the bulky Y300 side chain may additionally clear the TM6/TM7 interface. On the other hand, diminishing the volume of the side chain in position 251, such as in F251N, may also have some effect on constitutive activity both in the wild type and in the NQ background. Accordingly, we may expect that the novel designed mutants L127A, F254A, Y300A, L127A/Y300A, F254A/Y300A, F251N, NQ-F251N, NQ-Y300A, and NQ-F251N/Y300A would potentially display constitutive activity.

The above considerations were based on qualitative estimations; Figure 2 shows the final results of molecular modeling for each of the designed mutants together with the results obtained for WT,

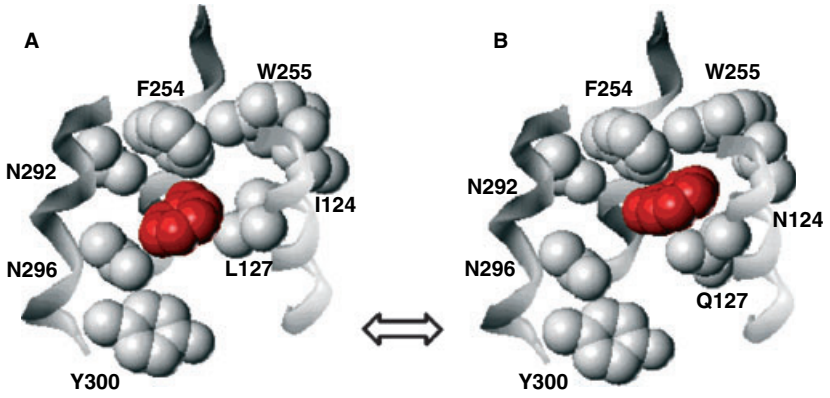


**Figure 1:** 3D model structures. Sketch of the conformations of the wild-type C5aR (A) and the constitutively active mutant NQ (B) differing by rotamers of the side chain of F251 (shown in red). Only side chains of the labeled residues are shown. The side chain of all residues except F251 are shown in white shades. Fragments of TM3, TM6, and TM7 are shown as white-shaded ribbons.

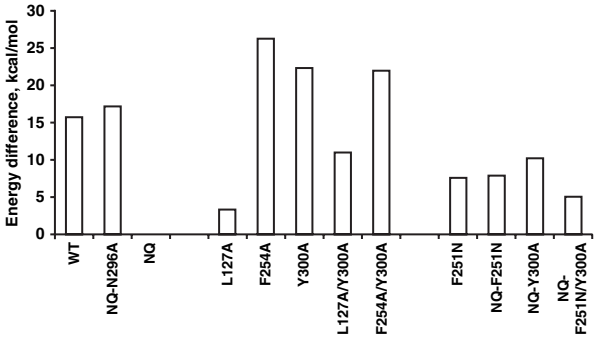


**Figure 2:** Energy landscape. Differences in energies (kcal/mol) between 3D structures of the C5a receptors corresponding to two different rotamers of the F251 side chain.

NQ, and NQ-N296A. Each bar in Figure 2 represents difference in conformational energies, $\Delta E$, calculated for a given receptor, assuming that the side chain of F251 occupies spatial positions corresponding to those depicted either in Figure 1A ('non-CAM' position, *g*– rotamer) or in Figure 1B ('CAM' position, *t* rotamer), while all other side chains are repacked (see Methods). Note that despite including the dihedral angles of the F251 side chain in the energy minimization (but not in the side chain repacking), no transitions were observed between the two rotamers during minimization. Also, changes in spatial positions of residues other than F251 between the minimized 3D structures corresponding to *g*– versus *t* rotamers of F251 were very small with the corresponding rms values varying from 0.172 (for F251N) to 0.439 Å (for NQ-N296A), the rms values calculated involving all C$\alpha$, C$\beta$, and C$\gamma$ atoms.

One can see that for WT and NQ-N296A (non-CAMs) the energy differences were >15 kcal/mol, whereas for NQ (CAM) the difference was negligible (0.03 kcal/mol). Notably, the results obtained for NQ and NQ-N296A showed that replacement of the gating residue L127 by Q127 is not *per se* sufficient for stabilization of the position of F251 inside the pocket; the more general system of residue–residue interactions is to be involved in this stabilization.

Based on the energy differences, $\Delta E$, the designed mutants may be roughly divided into two more or less distinct parts as potential CAMs and non-CAMs. Specifically, the results in Figure 2 predicted that within the group of mutants designed to facilitate the entry of the F251 side chain in the pocket, L127A and L127A/Y300A would more likely display constitutive activity, while F254A, Y300A, and F254A/Y300A would be non-CAMs. Regarding the mutants in the NQ background or mutation F251N, all were predicted to be possible CAMs, though, perhaps, with lower basal activity compared to that of NQ.

### *Site-directed mutagenesis*

Each of the mutant receptors was constructed by site-directed mutagenesis, expressed in mammalian COS-7 cells, and the ligand-stimulated or basal activities assessed by measuring $IP_3$ accumulation. The results are illustrated in Figure 3A. The wild-type receptor demonstrated low basal activity and relatively robust $IP_3$ accumulation upon ligand stimulation. For comparison, the NQ receptor showed about 2.5-fold increase in the basal signaling relative to the wild-type

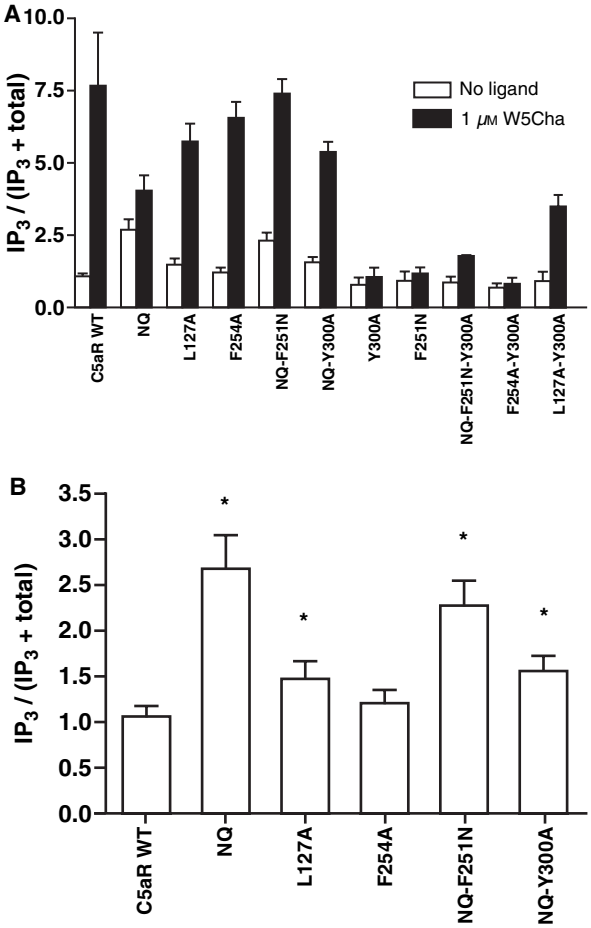


**Figure 3:** Results of biological testing in the mammalian cells. (Panel A) COS cells were transiently transfected with G$\alpha_{16}$ plus the wild type or mutants and treated with 1 $\mu$M W5Cha (black bars). Data represents the mean of three independent trials, +SD. The white bars represent basal activity of the wild type and the mutant receptors expressed in mammalian cells. (Panel B) Constitutive activity for the mutants that showed functional activity (ligand activation) in mammalian cells. Displayed are average figures from four of more experiments carried out in duplicates or quadruplicates. Asterisks denote $p < 0.05$, relative to the basal activity of the C5aR WT.

receptor, which is consistent with previous studies [e.g. threefold increase found earlier (21,24)]. The designed mutants L127A, F254A, NQ-F251N, and NQ-Y300A also displayed $IP_3$ accumulation upon ligand stimulation at the level not <0.5 of that for WT (Figure 3A).

Figure 3B represents the basal activities of the above four mutants together with WT and NQ. Three of the designed mutants, L127A, NQ-F251N, and NQ-Y300A, showed constitutive activity in the mammalian system exceeding that of the wild-type receptor in all experiments. Specifically, the levels of basal activity were as follows (normalized to the WT): NQ, 2.50 ± 0.22 (number of experiments = 4); L127A, 1.57 ± 0.21 ($n$ = 4); F254A, 1.00 ± 0.14 ($n$ = 4); NQ-F251N, 2.08 ± 0.20 ($n$ = 4); and NQ-Y300A, 1.34 ± 0.21 ($n$ = 4). Not surprisingly, the mutants that did not respond to ligand also did not show any increase in basal signaling levels: Y300A,

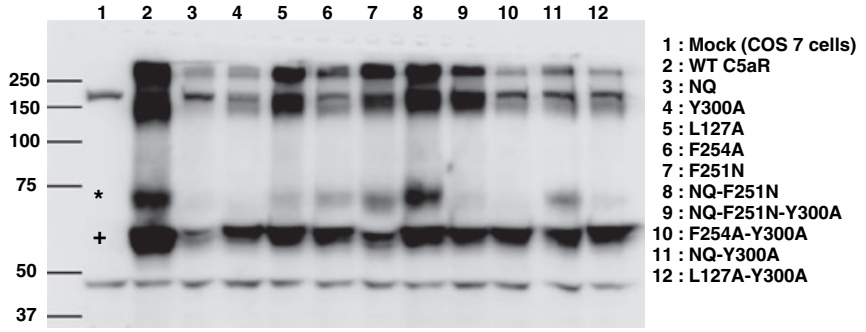


**Figure 4:** Western blot for expression of the wild type and mutant constructs. Western blot on whole cell extracts from COS cells expressing the wild-type and mutant receptors. The samples were separated on a 12% SDS-PAGE, blotted onto nitrocellulose membrane, and probed with C5aR antibody (see Materials and methods). Asterisks represent the complex oligosaccharides which traverse to the plasma membrane and (+) represents the high-mannose oligosaccharides which are sensitive to EndoH treatment and are generally hung up in the internal compartments. The Western blot is a representative experiment from one of the transfections that was used for the inositol phosphate assay.

0.82 ± 0.10 ($n$ = 2); F251N, 0.79 ± 0.08 ($n$ = 2); NQ-F251N-Y300A, 0.86 ± 0.03 ($n$ = 2); F254A-Y300A, 0.71 ± 0.07 ($n$ = 2); and L127A-Y300A, 0.82 ± 0.05 ($n$ = 2).

To further characterize the mutant C5aRs, we investigated the levels of expression for the mutant receptors (Figure 4). The expression levels of each mutant C5aR varied, and the CAMs (lanes 5, 8, and 11) had lower levels of overall expression than that of the wild-type receptor (lane 2), when the immunoreactivity is compared with the corresponding lanes. Earlier, we have observed in case of the wild-type receptor that the band corresponding to about 75 kDa (marked by an asterisk in Figure 4) represents the complex N-linked oligosaccharides insensitive to EndoH treatment (25) thus representing a fraction of the receptor which reaches the plasma membrane. Another fraction was presumably kept in the internal compartments, such as endoplasmic reticulum (ER), which is evidenced by the band marked (+) in Figure 4. Based upon this analysis, a fraction of the expressed mutants L127A, F254A, F251N, NQ-F251N, NQ-Y300A, and L127A-Y300A were correctly folded, and traversed to the plasma membrane. With the exception of F251N, these mutant receptors also displayed noticeable ligand stimulation and showed functional ligand binding (compare Figure 3A, black bars, and Figure 4). Conversely, several mutant receptors (Y300A, NQ-F251N-Y300A, F254A-Y300A; lanes 4, 9, and 10; Figure 4) migrate as high mannose-containing receptors, and thus did not appear to fold well enough to traverse to the plasma membrane. A low expression level for NQ (lane 3 in Figure 4) was observed as much of the receptor was internalized for this mutant and was not detected easily. This phenomenon was not investigated in detail for the CAMs L127A, NQ-F251N, and NQ-Y300A, but green fluorescence levels of the GFP-tagged receptors were qualitatively comparable with that of wild type as unlike in case of NQ (data not shown).

The above findings were supported also with the data obtained from competition-binding studies with $^{125}$I-labeled C5a ligand (see Table 1). The wild-type C5aR demonstrated two populations of binding activity: a smaller number of high affinity-binding sites (8.8–19.3 pmol/mg of receptors with $K_{d1}$ of 0.67–1.05 nM) and a larger number of low-affinity sites (3.0–5.7 nmol/mg of receptors with $K_{d2}$ of 163–400 nM). The presence of a large fraction of lower affinity sites has been reported for many GPCRs including the C5aR (26). The high-affinity sites are promoted by coupling to G proteins, while the low-affinity receptors likely represent uncoupled receptors and receptors that reside in the ER (J. M. Klco, S. Sen, and T. J. Baranski, unpublished data). As we have published previously (19,21), the NQ receptors demonstrated a smaller number of sites with higher affinity for ligand (0.69–13.9 pmol/mg with $K_{d1}$ of *ca.* 0.05–0.197 nM) relative to WT receptor. Regarding the L127A, the number of high-affinity sites is lower than for the WT C5aR (0.03–3.04 pmol/mg versus 8.8–13.7 pmol/mg, respectively) while the affinity is slightly higher than that for the WT receptor.

**Table 1:** Binding parameters for the wild type and mutant constructs

| | High-affinity sites | | Low-affinity sites | |
|---|---|---|---|---|
| Construct | $K_{d1}$ (nM) | $B_{max1}$ (pmol/mg) | $K_{d2}$ (nM) | $B_{max2}$ (nmol/mg) |
| C5aR WT | 1.05 ± 0.07 | 13.7 | 440 ± 45 | 5.70 |
| | 0.67 ± 0.01 | 8.8 | 305 ± 26 | 4.21 |
| | 1.05 ± 0.08 | 19.3 | 163 ± 54 | 3.00 |
| NQ | 0.05 ± 0.01 | 4.9 | 151 ± 75 | 1.62 |
| | <0.001 | 0.69 | 53.4 ± 4.9 | 0.47 |
| | 0.197 ± 0.041 | 13.9 | 143 ± 20 | 10.14 |
| L127A | 0.267 ± 0.202 | 3.04 | 830 ± 31 | 9.50 |
| | <0.001 | 0.03 | 884 ± 18 | 6.08 |
| NQ-F251N | N.A. | N.A. | 188 ± 11 | 2.76 |
| | | | 254 ± 16 | 1.99 |
| NQ-Y300A | N.A. | N.A. | 784 ± 26 | 3.69 |
| | | | 260 ± 22 | 2.91 |
| F254A | N.A. | N.A. | 1390 ± 200 | 10.8 |
| | | | 3460 ± 90 | 4.94 |
| F251N | N.A. | N.A. | 2000 ± 270 | 1.51 |
| | | | 6770 ± 250 | 2.46 |

Apparent $K_d$ values and approximate relative $B_{max}$ were directly derived from the raw data of the homologous competition-binding assay by fitting into two-site competition-binding models and taking the best fit $R^2$ values. Values are represented from each experiment, where the experiments have been repeated two to three times at least in duplicates and the SE values are representative of the data from within the experiment.
N.A., only single low-affinity sites were demonstrated for those receptors.

NQ-F251N and NQ-Y300A both demonstrated only single low-affinity sites at receptor numbers similar to the low-affinity WT-C5aR sites. The significance of only lower affinity sites is unclear and our results do not exclude a small population of high-affinity sites that could not be detected in these assays. Also, we did notice some variability in the binding data between sets of transfections. In case of NQ-F251N, from Figure 4, we observe that a significant fraction of this receptor has complex oligosaccharides and is likely present in the plasma membrane. The apparent discrepancy between the Western blot and the binding data are hard to explain. It is most likely that in this case, the receptor is not able to adapt itself in the high-affinity conformation and thus we observe only a single population. In case of F251N, a similar fraction of the receptors reach the plasma membrane, when compared to wild-type receptor (Figure 4, lane 7 versus lane 2). Despite this apparent normal folding and trafficking, the F251N mutant did not show either ligand-stimulated or CAM activity. The binding affinity of the ligand for the F251N is also relatively weak with the apparent $K_d$ values of 2000–7000 nM. Interestingly, the NQ-F251N receptor displays near normal activity in response to ligand (Figure 3A) and is also able to bind the ligand with a higher affinity compared to F251N. Thus, mutations in TM3 can rescue the defect imparted by the F251N mutation.

Finally, F254A and F251N also demonstrated a single low-affinity population of receptors that had lower affinity for C5a ligand relative to the WT-C5aR. Interestingly, F254A shows good signaling in response to agonist stimulation (Figure 3A) while F251N did not signal despite similar binding and expression levels relative to F254A.

## Discussion

Based on our energy calculations, the mutant receptors L127A, L127A/Y300A, F251N, NQ-F251N, NQ-Y300A, and NQ-F251N-Y300A were predicted as potentially CAMs, whereas receptors F254A, Y300A, and F254A-Y300A were predicted as potentially non-CAMs. Four of the designed mutants, namely L127A, F254A, NQ-F251N, and NQ-Y300A also displayed $IP_3$ accumulation upon ligand stimulation at the level not <0.5 of that for WT. The constitutive activity for all of the above four receptors was predicted correctly. Specifically, L127A, NQ-F251N, and NQ-Y300A showed basal activity higher than that of WT. Of note, for F254A the energy calculations demonstrated an even greater energy difference $\Delta E$ between the two states based on the position of the F251 side chain and predicted that this mutation should not result in a CAM. The calculation result is counterintuitive because qualitative inspection of the model of the TMs would suggest the reducing the size of the F254 would promote movement of the F251 side chain inside the pocket gated by F254 and L127. The experimental result confirmed the computational prediction underscoring the need for a quantifiable method of assessing the effects of potential mutations.

At the same time, our modeling showed that the same replacements, L127Q and I124N in two different mutants, NQ and NQ-N296A, result in different energetically preferable rotamers of F251, namely *t* in one case, and *g*– in the other. It may suggests that stabilization of the position of the F251 side chain inside the pocket depends mostly not from the size of the gating residues alone (and, consequently, not from the energy barrier between the two positions of the side chain of F251) but rather from the general system of residue–residue interactions within a specific mutant receptor. This agrees with the observation that differences in energies calculated only for interactions between TM helices directly surrounding F251, i.e. TM3, TM6, and TM7 ($\Delta E_{367}$), were not as predictive as energy differences calculated for the entire TM helical bundles in Figure 2. Specifically, the $\Delta E_{367}$ values for WT, NQ, L127A, F254A, NQ-F251N, and NQ-Y300A (the receptors represented in Figure 3B) were 4.1 kcal/mol, −4.9 kcal/mol, 0.9 kcal/mol, 8.4 kcal/mol, 9.1 kcal/mol and 3.8 kcal/mol, respectively, which most likely would leave NQ-F251N and NQ-Y300A predicted as non-CAMs contrary to experimental data.

Interestingly, the constitutive activity of the mutant NQ-F251N was of somewhat lower intensity than NQ, which may indicate a way to diminish basal activity in the constitutively active background. Also, the intensity of constitutive activation for NQ-Y300A was much lower than that of NQ. In this case, when we introduce the Y300A mutation in the NQ background thus eliminating the bulky group, the side chain of F251 potentially can move toward the TM6/TM7 interface hence decreasing and turning off the constitutive activity. It is important to note, however, that our modeling results were based on the tacit assumption that all designed mutants are able to fold properly in the 3D structure corresponding to the rhodopsin-like R state. At the same time, our experimental results showed that not all mutant receptors were functional upon ligand stimulation. The apparent discrepancy between the computational prediction and experimental data may also be due to inaccuracy of the computational score function (energy). For functional receptors, one can be sure that they are properly folded and available at the cell membrane surface (functionality is also evidenced by ligand-binding data); for others, one cannot exclude the improper folding, which could not be foreseen in current molecular modeling studies.

The results of our molecular modeling studies agree with the proposed crucial role of F251 as a focal point in the network of interactions between the TM3, TM6, and TM7 helices located deeply inside the TM core of the C5a receptor (22), which allowed design of new CAMs by modifications of residues contacting F251. Similar focal point located deeply inside the TM core occupies, according to our previous studies, the N111 residue in the TM3 helix of the angiotensin receptor type 1 (17). Elimination of the N111 side chain (such as in N111A or N111G) leads to the pronounced constitutive activity (4). Changes in constitutive activity due to elimination of the side chains of the residues directly or indirectly contacting N111, such as in the double mutants N111G/L112A or N111G/F117A, were correctly predicted by molecular modeling (17). It suggests that determining the focal points of interactions of functionally important residues by site-directed (such as in the angiotensin receptor type 1) or random (such as in the C5a receptor) mutagenesis in conjunction with independent molecular modeling studies may create a powerful tool for rational design of the novel CAMs of GPCRs.

It is noteworthy that our predictions were based on molecular modeling employing 3D models of the resting states of the C5a

receptors, and not on the 3D models of the activated state(s), which is(are) still unknown. In this regard, elucidation of the 'conformational switch' that regulates display of constitutive activity in the discussed mutants should be considered as the important initial step toward the general activation mechanism, which may include rotations of the TM helices around their long axis.

Finally, we note that this study presents a case where the hypothesis was made that the side chain movement of F251 was the 'hot spot', which might influence constitutive activity in case of C5aR. The constitutively active receptors have been very useful as experimental tools (27–29) for exploring varied functionalities in the area of academics as well as in industrial domain. Experimental analysis revealed that the design of the CAMs of a GPCR directly based on predictions from molecular modeling agreed with the hypothesis. This will in turn help us better understand how GPCRs function at the molecular level.

## Acknowledgment

This work was partly funded by the NIH grants 63720 (T.J.B.), 71634 (T.J.B. and G.V.N), and 68460 (G.V.N.).

## References

1. Fredriksson R., Lagerstrom M.C., Lundin L.G., Schioth H.B. (2003) The G-protein-coupled receptors in the human genome form five main families. Phylogenetic analysis, paralogon groups, and fingerprints. Mol Pharmacol;63:1256–1272.
2. Gether U. (2000) Uncovering molecular mechanisms involved in activation of G protein-coupled receptors. Endocrin Rev;21:90–113.
3. Drews J. (2000) Drug discovery: a historical perspective. Science;287:1960–1964.
4. Parnot C., Bardin S., Miserey-Lenkei S., Guedin D., Corvol P., Clauser E. (2000) Systematic identification of mutations that constitutively activate the angiotensin II type 1a receptor by screening a randomly mutated cDNA library with an original pharmacological bioassays. Proc Natl Acad Sci USA;97:7615–7620.
5. Parnot C., Miserey-Lenkei S., Bardin S., Corvol P., Clauser E. (2002) Lessons from constitutively active mutants of G protein-coupled receptors. Trends Endocrinol Metab;13:336–343.
6. Nikiforovich G.V., Marshall G.R. (2006) 3D modeling of the activated states of constitutively active mutants of rhodopsin. Biochem Biophys Res Commun;345:430–437.
7. Ladds G., Davis K., Das A., Davey J. (2005) A constitutively active GPCR retains its G protein specificity and the ability to form dimers. Mol Microbiol;55:482–497.
8. Schutz W., Freissmuth M. (1992) Reverse intrinsic activity of antagonists on G protein-coupled receptors. Trends Pharmacol Sci;13:376–380.
9. Lefkowitz R.J., Cotecchia S., Samama P., Costa T. (1993) Constitutive activity of receptors coupled to guanine nucleotide regulatory proteins. Trends Pharmacol Sci;14:303–307.
10. Scheer A., Cotecchia S. (1997) Constitutively active G protein-coupled receptors: potential mechanisms of receptor activation. J Recept Signal Transduct Res;17:57–73.
11. Pauwels P.J., Wurch T. (1998) Review: amino acid domains involved in constitutive activation of G-protein-coupled receptors. Mol Neurobiol;17:109–135.
12. Leff P. (1995) The two-state model of receptor activation. Trends Pharmacol Sci;16:89–97.
13. Gether U., Kobilka B.K. (1998) G protein-coupled receptors: II. Mechanism of agonist activation. J Biol Chem;273:17979–17982.
14. Kenakin T. (2001) Inverse, protean, and ligand-selective agonism: matters of receptor conformation. FASEB J;15:598–611.
15. Seifert R., Wenzel-Seifert K. (2002) Constitutive activity of G-protein-coupled receptors: cause of disease and common property of wild-type receptors. Naunyn Schmiedebergs Arch Pharmacol;366:381–416.
16. Nikiforovich G.V., Galaktionov S., Balodis J., Marshall G.R. (2001) Novel approach to computer modeling of seven-helical transmembrane proteins: current progress in test case of bacteriorhodopsin. Acta Biochim Pol;48:53–64.
17. Nikiforovich G.V., Mihalik B., Catt K.J., Marshall G.R. (2005) Molecular mechanisms of constitutive activity: mutations at position 111 of the angiotensin $AT_1$ receptor. J Pept Res;66:236–248.
18. Baranski T.J., Herzmark P., Lichtarge O., Gerber B.O., Trueheart J., Meng E.C., Iiri T. *et al.* (1999) C5a receptor activation. Genetic identification of critical residues in four transmembrane helices. J Biol Chem;274:15757–15765.
19. Gerber B.O., Meng E.C., Dotsch V., Baranski T.J., Bourne H.R. (2001) An activation switch in the ligand binding pocket of the C5a receptor. J Biol Chem;276:3394–3400.
20. Matsumoto M.L., Narzinski K., Kiser P.D., Nikiforovich G.V., Baranski T.J. (2007) A comprehensive structure-function map of the intracellular surface of the human C5a receptor: I. Identification of critical residues. J Biol Chem;282:3105–3121.
21. Whistler J.L., Gerber B.O., Meng E., Baranski T.J., von Zastrow M., Bourne H.R. (2002) Constitutive activation and endocytosis of the complement factor 5a receptor: evidence for multiple activated conformations of a G protein-coupled receptor. Traffic;3:866–877.
22. Hagemann I.S., Nikiforovich G.V., Baranski T.J. (2006) Comparison of the retinis pigmentosa mutations in rhodopsin with a functional map of the C5a receptor. Visual Res;46:4519–4531.
23. Nikiforovich G.V., Hruby V.J., Prakash O., Gehrig C.A. (1991) Topographical requirements for delta-selective opioid peptides. Biopolymers;31:941–955.
24. Klco J.M., Wiegand C.B., Narzinski K., Baranski T.J. (2005) Essential role for the second extracellular loop in C5a receptor activation. Nat Struct Mol Biol;12:320–326.
25. Klco J.M., Nikiforovich G.V., Baranski T.J. (2006) Genetic analysis of the first and third extracellular loops of the C5a receptor reveals an essential WXFG motif in the first loop. J Biol Chem;281:12010–12019.
26. Gerard N.P., Hodges M.K., Drazen J.M., Weller P.F., Gerard C. (1989) Characterization of a receptor for C5a anaphylatoxin on human eosinophils. J Biol Chem;264:1760–1766.

27. Konopka J.B., Margarit S.M., Dube P. (1996) Mutation of Pro-258 in transmembrane domain 6 constitutively activates the G protein-coupled alpha-factor receptor. Proc Natl Acad Sci USA; 93:6764–6769.
28. Alewijnse A.E., Timmerman H., Jacobs E.H., Smit M.J., Roovers E., Cotecchia S., Leurs R. (2000) The effect of mutations in the DRY motif on the constitutive activity and structural instability of the histamine H(2) receptor. Mol Pharmacol;57:890–898.
29. Decaillot F.M., Befort K., Filliol D., Yue S., Walker P., Kieffer B.L. (2003) Opioid receptor random mutagenesis reveals a mechanism for G protein-coupled receptor activation. Nat Struct Biol;10:629–636.